PHYSICAL REVIEW B **72**, 104301 (2005)

Ion hopping in crystalline and glassy spodumene $LiAlSi_2O_6$: ^7Li spin-lattice relaxation and ^7Li echo NMR spectroscopy

F. Qi, C. Rier, and R. Böhmer*
Experimentelle Physik III and Interdisziplinäres Zentrum für Magnetische Resonanz, Universität Dortmund, 44221 Dortmund, Germany

W. Franke and P. Heitjans†
Institut für Physikalische Chemie und Elektrochemie, Universität Hannover, 30167 Hannover, Germany
(Received 13 December 2004; revised manuscript received 26 April 2005; published 15 September 2005)

Nuclear magnetic resonance spectroscopy was used to study polycrystalline β-spodumene (β-$LiAlSi_2O_6$) as well as glassy specimens with the same chemical composition. ^7Li spin-lattice relaxation measurements were carried out in a broad temperature range and for several Larmor frequencies. In addition to a pronounced rate maximum at high temperatures, stemming from the long-range Li motion in these aluminosilicates, we found a weak maximum in the crystalline modification near 120 K. The latter result confirms the existence of a local double-well structure in which the Li ions reside. The ionic motion was also monitored by solid- and stimulated-echo spectra as well as by the decay of the Jeener-Broekaert echo. Under conditions which are discussed in detail, the latter is a direct measure of the hopping correlation function. For the glass this function was found to decay faster and more stretched than that of the crystal at a given temperature. Furthermore, the relevant barriers against the high-temperature long-range Li motion are larger in the crystal as compared to the glass.

DOI: 10.1103/PhysRevB.72.104301 PACS number(s): 66.30.Hs, 76.60.−k

I. INTRODUCTION

Lithium aluminosilicates with the composition $Li_2O \cdot Al_2O_3 \cdot nSiO_2$ include as crystalline representatives the minerals eucryptite ($LiAlSiO_4$), spodumene ($LiAlSi_2O_6$), and petalite ($LiAlSi_4O_{10}$).[1] The corresponding glasses with $n=2$, 4, and 8 are easily produced from the melt. Glass ceramics, in particular those with the spodumene composition ($n=4$), find widespread application as tailored materials with negligible thermal expansion due to the fact that the glass and its crystalline counterpart have thermal expansion coefficients with opposite signs.[2] From a more fundamental point of view, $Li_2O \cdot Al_2O_3 \cdot nSiO_2$ has been used as a model system to study the dependence of ion (Li^+) movement and conduction on the extent of structural order or disorder. The properties of polycrystalline and of amorphous material with the same chemical composition were, e.g., explored in comparative studies on $LiAlSi_2O_6$ glass and β-spodumene (β-$LiAlSi_2O_6$) polycrystals using NMR and conductivity spectroscopy.[3,4] In the present article we focus on ^7Li NMR, which is a valuable tool for the study of dynamics in various ion conducting materials; for reviews see, e.g., Refs. 5 and 6.

The high-temperature phase β-$LiAlSi_2O_6$ is a stuffed derivative of the quartz structure known as keatite and has the tetragonal space group $P4_32_12$ (or $P4_12_12$).[7,8] The structure consists of a three-dimensional aluminosilicate framework. One-third of the silicon atoms is replaced by aluminum atoms at random. The charge of an AlO_4^- group is in each case compensated by a lithium ion. The structure shows zeolite like channels. The channels parallel to both the a and b axes have a free diameter of about 3 Å and are appreciably wider than those parallel to the c axis. There are four sets of paired sites for Li atoms per unit cell. Each Li atom occupies one of the two sites in each pair. The distance between the two sites is only 0.13 nm, which is too short for the Li atoms to occupy both simultaneously. The distance from a pair of sites to the next pair is about 0.45 nm.

From the structure it appears that there are essentially two different possible Li jump processes: long-range jumps from one pair of Li sites to the next and a localized motion by hops between the sites of a pair. Some aspects of the former process were already studied in earlier NMR work.[3] There the spin-lattice relaxation rate T_1^{-1} of ^7Li was measured from 150 K up to 930 K in the glass (which is slightly below the glass transition temperature $T_g \approx 960$ K) and up to 1300 K in the polycrystalline material at various Larmor frequencies in the range from 10 to 100 MHz. Pronounced $T_1^{-1}(T)$ maxima were found at various temperatures, depending on the Larmor frequency, in the regime from about 650 to 850 K and were attributed to long-range jumps in glassy and crystalline spodumene. One goal of the present paper is to study also the localized Li ion motion systematically by spin-lattice relaxation rate measurements, extending previous results to lower temperatures and higher frequencies. Further additional T_1^{-1} data in the high-temperature range will be presented. While spin-lattice relaxation is most sensitive to relatively fast motions with motional correlation times close to the inverse Larmor frequencies, echo techniques are generally more sensitive to slower motions. To investigate the dynamics in the time window of microseconds and longer we employ solid- and stimulated-echo spectroscopy as well as the decay of the Jeener-Broekaert echo.

Concerning other investigations in glassy and crystalline spodumene performed hitherto, we mention that the spin-lattice relaxation rate of the β emitter ^8Li was measured[9] down to temperatures of $T=12$ K using β-radiation-detected NMR (β-NMR). Here the probe nuclei are produced and spin polarized *in situ* by the capture of polarized neutrons.[10]

While this study is aimed at dynamical processes, structural characterization was performed via ^{29}Si and ^{27}Al solid-state NMR spectra as well as via positron annihilation lifetime spectroscopy.[11,12] Impedance measurements have been presented and discussed by various authors—e.g., Refs. 4 and 13–15. For lithium aluminosilicates the issue of comparing motional correlation times obtained from NMR and from conductivity measurements was dealt with in, e.g., Refs. 4 and 16–18. We further mention a computer simulation study of Li ion migration in the β-spodumene structure.[19]

This paper is organized as follows: First, we will review some features of the echo spectroscopy used in this work and then in Sec. III we describe the experimental details. The results of our experiments are subsequently presented, analyzed, and discussed in Sec. IV. Here we will first deal with the spin-lattice relaxation and then with the solid-echo and stimulated-echo spectra. This section is followed by a description of the evolution and the mixing time dependence of the stimulated echo that we will synonymously call the Jeener-Broekaert-echo in this article. Near the end of Sec. IV the results for the Li motional correlation times of the glassy and the crystalline samples are compared. Finally, in Sec. V we summarize our findings.

II. ^{7}Li SOLID-ECHO AND STIMULATED-ECHO SPECTROSCOPY

For our measurements we used standard relaxometry techniques, in addition to the solid-echo as well as the Jeener-Broekaert-echo method.[20] The latter, apart from an early application,[21] has only recently been used to study the ultraslow dynamics of Li ion conductors.[22–25] In the following, we briefly summarize some theoretical aspects concerning the echo techniques in nonrotating samples. Considerations relevant to experiments carried out under conditions of magic angle spinning will not be considered here.[26]

The systematic time evolution of the ^{7}Li spins in nonspinning samples is typically governed by the first-order quadrupolar Hamiltonian[27]

$$\hat{H}_Q = \frac{\omega_Q}{6}[3\hat{I}_z\hat{I}_z - I(I+1)]. \tag{1}$$

Here $\omega_Q = \frac{1}{2}\delta_Q(3\cos^2\theta_Q - 1 - \eta_Q \sin^2\theta_Q \cos 2\phi_Q)$ designates the quadrupolar precession frequency in the rotating frame and $\delta_Q = \frac{1}{2}eqeQ/\hbar$ is the anisotropy parameter for a nucleus with spin quantum number $I=3/2$. η_Q denotes the so-called asymmetry parameter, and θ_Q and ϕ_Q specify the orientation of the electrical field gradient tensor at the Li site with respect to the external static magnetic field.

Solid-echo spectra can be generated using the sequence $X_{90°}$-t_p-Y_{β_2}-t-acquisition and subsequent Fourier transformation. Here t_p denotes the evolution time, β_2 the flip angle of the second pulse, and t the detection time. Using a straightforward density matrix calculation,[27] which neglects spin-relaxation effects, the detectable signal intensity is given by the trace of the density operator $\hat{\rho}$ with the appropriate spin operator component. This was chosen here as $\hat{I}_y$, since the trace with $\hat{I}_x$ vanishes. One obtains

$$\begin{aligned}\mathrm{Tr}[\hat{\rho}(t)\hat{I}_y] = \frac{1}{20}\{&-5 - 9\cos(\omega_Q t_p)\cos(\omega_Q t)\\ &- 3\cos(\omega_Q t_p) - 3\cos(\omega_Q t) - 3\cos(2\beta_2)\\ &\times[1 + \cos(\omega_Q t_p)\cos(\omega_Q t) - \cos(\omega_Q t_p)\\ &- \cos(\omega_Q t) - 4\sin(\omega_Q t_p)\sin(\omega_Q t)]\}.\end{aligned} \tag{2}$$

The detectable time-domain signal is written here to emphasize the dependence on the second flip angle β_2. If Eq. (2) is regrouped, it is possible to identify three contributions: one which does not depend on the detection time t, one which depends on $\cos(\omega_Q t)$, and one which depends on $\sin(\omega_Q t)$. After Fourier transformation with respect to the detection time t these contributions yield the intensity of the central component $I_C(t_p) = \frac{1}{20}[-5 - 6\cos(\omega_Q t_p)\sin^2\beta_2 - 3\cos(2\beta_2)]$, that of the satellites $I_S = \frac{1}{20}[-9\cos(\omega_Q t) - 6\sin^2\beta_2 - 3\cos(2\beta_2)\cos(\omega_Q t)]$, and an out-of-phase component $I_i = \frac{12}{20}\cos(2\beta_2)\sin(\omega_Q t)$, respectively. When $\omega_Q t_p \to 0$ the ratio I_C/I_S becomes

$$\lim_{\omega_Q t_p \to 0} \frac{I_C}{I_S} = \frac{2}{3},$$

i.e., independent of the second flip angle β_2. In real experiments a finite interpulse delay t_p has to be chosen to overcome finite receiver dead times. Under these circumstances the ratio I_C/I_S does depend on β_2. But for the experimentally relevant quadrupolar frequencies $\omega_Q \leqslant 2\pi \times 50$ kHz and $t_p = 20$ μs, the ratio deviates from its theoretically expected value by no more than 1% if one chooses $\beta_2 = 64°$. This result is in accord with a previous calculation, which takes the quadrupolar evolution during the pulses into account, but which focuses only on the $\eta_Q = 0$ case.[28] The approach of the present work does not refer to a particular choice of η_Q. This is important since in ^{7}Li solid-state NMR $\eta_Q = 0$ will only rarely be the case. We point out that our calculations are based on taking the Fourier transform of the entire time-domain signal. However, in the experiments discussed below the signal starting at the echo maximum was transformed.

Jeener-Broekaert echoes can be generated using the pulse sequence X_{β_1}-t_p-Y_{β_2}-t_m-X_{β_2}-t_p-acquisition. Under the sole perturbation of the first-order quadrupolar Hamiltonian a pure spin-alignment state can be generated during the mixing time t_m if proper phase cycling is employed.[29,30] The total signal corresponding to the three-pulse sequence then yields

$$\begin{aligned}&S_2(t_p, t_m, t)\\ &\quad = \tfrac{9}{20}\sin\beta_1 \sin 2\beta_2 \sin 2\beta_3 \sin[\omega_Q(0)t_p]\sin[\omega_Q(t_m)t],\end{aligned} \tag{3}$$

which, after Fourier transformation with respect to the acquisition time t, gives rise to a pure satellite spectrum. If, in addition to Eq. (1), homonuclear dipolar interactions among the ^{7}Li spins are included, additional signal contributions can arise.[24] In particular spectral components with frequencies close to zero can then show up. A simplified calculation of these effects demonstrated that central and satellite components may not always be characterized by the same apparent

phases.[24] The spin-alignment state is in addition subject to longitudinal relaxation processes which are not included in Eq. (3). These as well as changes in the precession frequencies can be monitored by varying the mixing time t_m. In Eq. (3) these frequencies are correlated essentially at two points in time. A higher-order characterization, which is possible using three- and four-time stimulated-echo techniques also for ^{7}Li systems,[30,31] was not attempted in the present work.

Within a simple two-spin approximation it was shown that in the presence of homonuclear ^{7}Li dipolar interactions the first two pulses of the Jeener-Broekaert sequence generate a superposition of product states $\Sigma_{l,l'} c_{ll'} T_{l0} T_{l'0}$ with even $L=l+l'$ (Ref. 24). Here T_{l0} denotes an irreducible spherical tensor operator of rank l and $c_{ll'}$ an expansion coefficient. For the discussion below it will be of relevance to recall that under the action of a hard rf pulse characterized by the propagator U_β these operators transform according to $U_\beta^{-1} T_{l0} U_\beta = \pm U_{180°-\beta}^{-1} T_{l0} U_{180°-\beta}$. Here the positive sign holds for odd l ("mirror symmetry" with respect to a flip angle of $\beta=90°$) and the negative one for even l. The latter condition, with l then replaced by L, also holds if the rotation of two-spin states is considered.

III. EXPERIMENTAL DETAILS

In the present work we studied glassy as well as crystalline specimens. The glassy material $Li_2O \cdot Al_2O_3 \cdot nSiO_2$ was prepared by mixing appropriate amounts of Li_2CO_3, Al_2O_3, and SiO_2, melting the mixture in a platinum crucible, and subsequent quenching of the melt either by roller quenching or by rapid cooling of the platinum container. The polycrystalline β-$LiAlSi_2O_6$ samples were taken from the batches studied previously or they were obtained by recrystallizing the glass as described in Ref. 3. We also prepared samples using ^{6}Li-enriched Li_2CO_3 (Eurisotop) in order to achieve ^{7}Li:^{6}Li ratios down to 1:3. Since this did not alter the width of the central NMR line significantly as compared to that of the samples with natural abundance, the spectra of these samples will not be discussed further in the present article.

For the measurements carried out at 46.1, 117.6, and 127.1 MHz, a previously employed homebuilt spectrometer was used. The experimental conditions for the NMR measurements have been described elsewhere.[22] Spin-lattice relaxation times were measured using an inversion recovery pulse sequence combined with a solid echo for detection. Below, we present also some previously unpublished T_1 measurements recorded at a Larmor frequency of 38.9 MHz; see also Ref. 3. For the latter measurements a Bruker MSL100 spectrometer was used together with a variable-field (0–7 T) Oxford magnet.

Solid-echo spectra were taken with an interpulse delay of 20 μs. For the spin-alignment spectra the first evolution time t_p and the mixing time t_m were both typically set to 10 μs. Unless otherwise stated the flip angles of the pulses were $\beta_1=90°$ and $\beta_2=\beta_3=45°$ with the 90° pulse typically being 3 μs long. For the phasing of all spectra a first-order phase correction was applied to minimize the dispersive part of the spectrum.

Below room temperature the measurements were carried out using cryostats from Oxford Instruments and from Cryovac. For the high-temperature experiments furnaces were used which are similar in design to those described elsewhere.[32] The long-term (days) temperature stability was about ±0.2 K in each case.

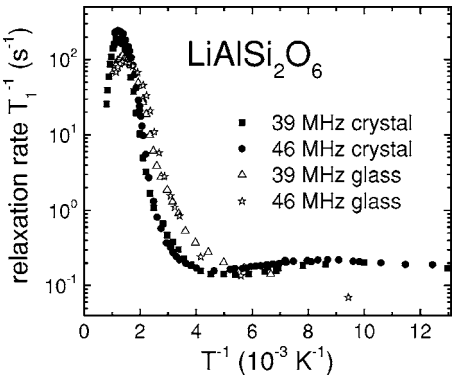

FIG. 1. Spin-lattice relaxation rate of polycrystalline and glassy spodumene as a function of the reciprocal temperature for two Larmor frequencies $\omega_L/2\pi$. Most of the data recorded at 39 MHz were taken from Ref. 3. The 46 MHz data are from the present work.

IV. RESULTS AND DISCUSSION

A. Spin-lattice relaxation

In Fig. 1 we compare the spin-lattice-relaxation rates of crystalline and of glassy spodumene as measured at Larmor frequencies of 38.9 and 46.1 MHz. Overall a broad temperature range from 40 to 1300 K is covered. Some aspects of the 38.9 MHz data acquired above room temperature which also include the regime of the high-temperature flank of the diffusion-induced peak were discussed previously.[3] The spin-lattice relaxation times recorded in the present work at somewhat higher Larmor frequencies nicely agree with the earlier ones. Therefore it may suffice to note that in the crystalline material the global maximum in T_1^{-1} occurs at a higher temperature and is considerably larger than in the glass. The temperature shift in the rate maximum is obviously due to the fact that the mean jump rate is smaller and the average potential barrier against ion migration is larger in the crystal than it is in the glass. According to the Bloembergen-Purcell-Pound (BPP) theory of spin-lattice relaxation[33] at a maximum of T_1^{-1}, the condition $\omega_L \tau_C = 0.62$ is fulfilled. For $\omega_L/2\pi = 38.9$ MHz this yields hopping correlation times of $\tau_C = 2.5$ ns at 700 and 820 K for the glass and crystal, respectively. The τ_C value is clearly only a rough estimate because, as evident from the asymmetry of the peak in $\log T_1^{-1}$ vs $1/T$ and as discussed in some detail in Ref. 3, spin-lattice relaxation shows non-BPP behavior. The activation energy E_a obtained from the slope of the low-temperature side of the T_1^{-1} peak is 0.50±0.02 eV for the crystal and 0.34±0.03 eV for the glass, neglecting a possible slight frequency dependence.[3,9] Since the ^{7}Li quadrupolar coupling constants are comparable for the two modifications (see the experiments presented in Fig. 5 below), the reduced T_1^{-1} maximum can be taken to indicate that the distribution of ionic hopping rates is broader in the glassy sample.

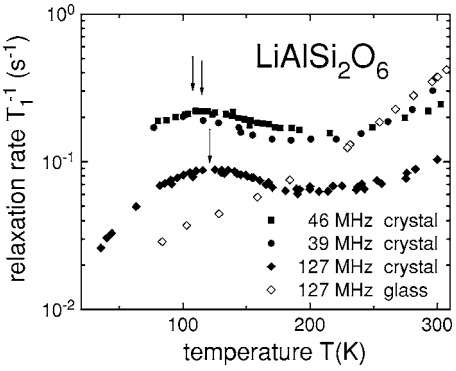

FIG. 2. Spin-lattice relaxation times for different Larmor frequencies are shown here as a function of temperature. This representation brings the maxima out more clearly than an inverse temperature plot. The solid symbols represent spin-lattice relaxation rates of crystalline β-spodumene. The T_1^{-1} maxima clearly depend on the Larmor frequency and thus allow one to extract typical correlation times $\tau_C \equiv (2\pi\nu_C)^{-1} = 0.62/\omega_L$. For the glass (open symbols) no maximum is seen in the temperature range shown in this figure.

At low temperatures the difference between the crystalline and the glassy material is more striking. While a significant local rate maximum shows up for the polycrystal somewhat above 100 K, such a feature seems to be absent in the present glass data (see Fig. 1). The relaxation rates in the temperature range below ambient, measured at three different Larmor frequencies, are plotted in Fig. 2 versus temperature. As expected for motion-induced rate maxima, their positions (indicated by the arrows in Fig. 2) shift to higher temperatures with the frequency increasing. A quantitative evaluation will be given below (see Fig. 3). The observation of a frequency-dependent rate maximum for the polycrystal is reminiscent of observations made for aluminosilicate glass ceramics with different degrees of crystallinity: A dielectric loss peak is clearly resolved in the ceramic specimen, but it is barely detectable in the precursor glass.[14] This finding was

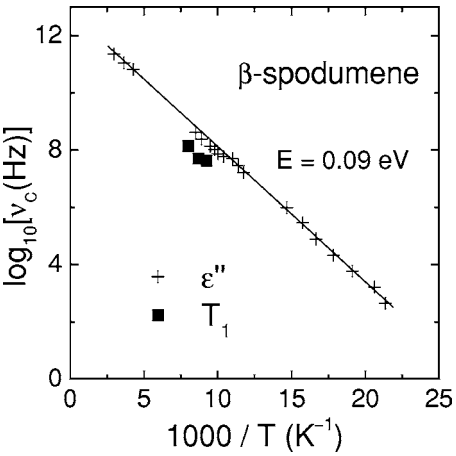

FIG. 3. Arrhenius plot of the correlation rates (divided by 2π) associated with the localized Li motion. The dielectric loss peak frequencies from Ref. 14 are compared with the frequencies ν_C that can be read off from Fig. 2. The solid line corresponds to an energy barrier of 0.09 eV.

interpreted to indicate that the well-defined double-well structure which characterizes the crystal may be largely absent or at least exhibit a large variability in the glass. It is noted, however, that in recent β-NMR measurements using the probe nucleus ^{8}Li it was found that not only crystalline β-spodumene but also the glassy counterpart exhibits a—albeit weak—T_1^{-1} maximum appearing as a shoulder in the relaxation data at temperatures below the prominent T_1^{-1} maximum due to long-range Li diffusion.[9] In these experiments the Larmor frequency was as low as 3 MHz.

The arguments utilized to compare the results from dielectric with those from NMR spectroscopy are based on an expression associating the dielectric loss ε'' on the scale of the Larmor frequency with a relaxation rate. The latter can be written as[34,35]

$$\frac{1}{T_1^{\mathrm{diel}}} \propto \frac{\varepsilon''(\omega_L) + 4\varepsilon''(2\omega_L)}{\omega_L \Delta\varepsilon}. \tag{4}$$

Here $\Delta\varepsilon$ designates the amplitude of the dielectric relaxation strength. In general, the relaxation rate $1/T_1^{\mathrm{diel}}$ will not exactly match the spin-lattice relaxation rate obtained from NMR since the two quantities are related to two somewhat different correlation functions which typically differ slightly, e.g., due to their different angular sensitivities.

In order to check the extent to which the maxima seen in the relaxation rate and in the dielectric loss correspond to one another, we have compiled both types of results in Fig. 3. Here we compare the dielectric loss peak frequencies $\nu_C = 1/(2\pi\tau_C)$ with the corresponding values from the spin-lattice relaxation rate maxima on the basis of the relation that $\omega_L\tau_C = 0.62$ (Ref. 33). The data from dielectric spectroscopy and those from NMR exhibit the same trend, implying that the two methods are sensitive to the same kind of local motion. The solid line through the dielectric data reflects an Arrhenius law $\nu_C = \nu_0 \exp(-E/k_B T)$ with an attempt frequency $\nu_0 = 7 \times 10^{12}$ Hz and an energy barrier of 0.09 eV as deduced from previous dielectric investigations.[14] The correlation rates of the local motion obtained by NMR are smaller than those from the dielectric data of the polycrystalline material, to which the comparison has to be confined in the present case (see Fig. 3). A similar, though somewhat larger, effect has previously been reported for various glasses and explained by different theoretical concepts comparing spin-lattice relaxation and conductivity in disordered materials; see Refs. 16, 17, and 36–38.

In the foregoing we discussed the overall spin-lattice relaxation behavior $\langle T_1 \rangle = \int M(t)\mathrm{d}t$ as estimated from the properly normalized longitudinal magnetization $M(t)$. For a spin system with $I = 3/2$ the magnetization in general reequilibrates in a nonexponential manner, even under conditions of nonselective excitation. If the relaxation is purely quadrupolar, then calculations[39] show that the satellites and the central line recover with different (combinations of) rates, so that the relaxation of the total magnetization is given by $M(t) \propto e^{-2W_1 t} + 4e^{-2W_2 t}$. Here the rates W_n are proportional to the spectral densities $J(n\omega_L)$ for $n = 1, 2$. Single-exponential relaxation is thus only expected in the limit of extreme narrowing for which $J(\omega_L) = J(2\omega_L)$.

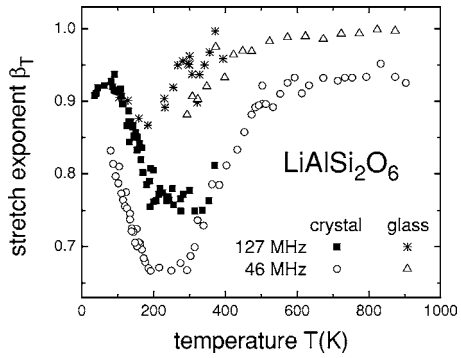

FIG. 4. Temperature dependence of the exponent β_T characterizing the stretching of the longitudinal magnetization recovery according to Eq. (5). At high temperatures spin-lattice relaxation is almost exponential ($\beta_T \approx 1$), at least for the glassy sample. The more complex behavior seen at lower temperatures is discussed in the text.

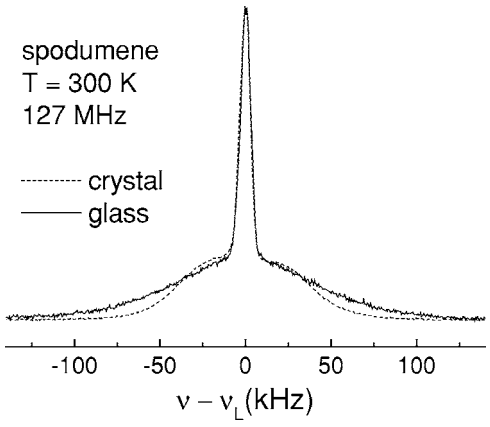

FIG. 5. Comparison of solid-echo spectra recorded at 127 MHz for crystalline and glassy spodumene employing a 90°-90° pulse sequence.

In the absence of a specific model for the relaxation mechanism it may be advisable to employ an alternative approach. Here we will use the stretched exponential function

$$M(t) \propto \exp[-(t/T_1)^{\beta_T}] \tag{5}$$

in order to obtain a phenomenological description. The Kohlrausch exponent β_T is a measure for the deviation from exponential magnetization recovery, and the mean relaxation time is given by $\langle T_1 \rangle = (T_1/\beta_T)\Gamma(1/\beta_T)$, with Γ denoting the gamma function. The temperature dependence of the exponent β_T is depicted in Fig. 4. At least for the glassy sample, it indicates an almost exponential decay at high temperatures.

With decreasing temperature, in the region of the local T_1^{-1} maxima, the exponents β_T decrease and show minima themselves. At the lowest temperatures $T < 200$ K, the exponents increase again. Similar to the situation in deuteron spin systems,[40] we may interpret this finding as an indication of the influence of spin diffusion. Here the apparent averaging is more effective; i.e., the spin-lattice relaxation is more exponential, the smaller $1/T_1$ is, and thus the closer these rates are to the (Larmor frequency independent) spin-diffusion rate. This argument rationalizes why the faster magnetization recoveries corresponding to lower Larmor frequencies can get more nonexponential (cf. Fig. 4): This is simply because averaging by dipolar interactions here is less effective.

B. NMR spectra

1. Solid-echo spectra

In Fig. 5 we show solid-echo spectra of polycrystalline and glassy spodumene recorded at room temperature using a 90°-90° pulse sequence. It is seen that the widths of the central transitions of the two spectra are identical. Within experimental error we find a full width at half maximum (FWHM) of the central component, $\Delta_C = 6$ kHz (Ref. 41). This obviously shows that the mean separation to the other nuclei and hence the strength of the dipolar interaction do not depend on the degree of long-range order. For the crystal the satellite part of the spectra exhibits an almost Gaussian shape with a FWHM of about $\Delta_S = 63$ kHz. The spectrum of the glassy sample exhibits a somewhat larger width (86 kHz). This reflects the larger distortion of the local Li^+ environments.

Upon increasing the temperature of the glassy and crystalline samples, the contribution of the satellites to the spectral shape steadily decreases and for 400 K $< T <$ 525 K and 500 K $< T <$ 550 K, respectively, the satellite contributions are barely discernible (not shown). As Fig. 6(a) shows at higher temperatures some quadrupolar intensity reappeared for the crystal (the glass was not measured for $T > 525$ K). It is seen that the spectra of the crystal become more and more structured upon heating. For temperatures above about 700 K a Pake-like powder pattern is clearly recognized. Motional processes lead to a rapid decay of the transverse magnetization if the average correlation time is of the order of the inverse quadrupolar coupling constant (roughly 10–50 μs). Therefore, for finite evolution times the quadrupolar intensity is expected to be smallest when the two time scales are comparable. Since in the glass the quadrupolar intensity gets small at lower temperature, this argument shows that ionic motion is faster in this compound.

Near 600 K an additional broad background signal is visible for the crystal, suggesting that at these temperatures the spectra exhibit a two-phase character. In order to support this hypothesis in Fig. 6(b) we show a spectrum which has been obtained by adding the solid-echo spectra recorded at 483 and 733 K with equal weights: This spectrum qualitatively agrees with the one recorded near 600 K. Analogous to other disordered systems,[42] the observation of two-phase spectra hints at the existence of a broad distribution of motional correlation times in the crystal.

Overall, the central line dominates the solid-echo spectra. Therefore we have also measured spin-alignment spectra in which the central component is largely suppressed.

2. Spin-alignment spectra

Spin-alignment spectra were recorded over a large temperature range from 152 to 833 K. Some representative

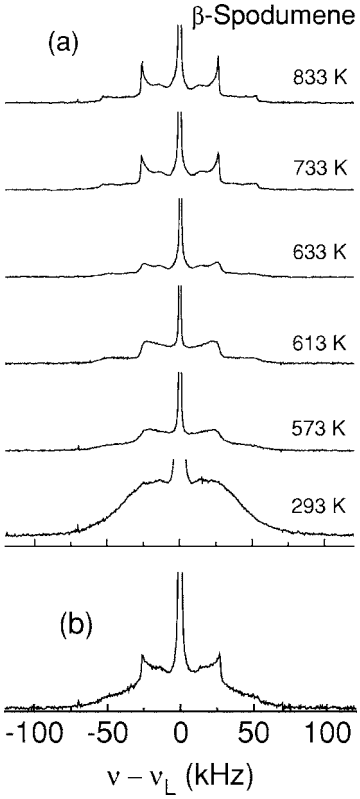

FIG. 6. (a) Solid-echo spectra of crystalline β-spodumene as measured using a 90°-64° sequence at 46.1 MHz for various temperatures. The spectra were scaled such that they all exhibit the same peak intensity and only the lowest 10% of each spectrum is shown. (b) Composite spectrum obtained by adding spectra taken at 483 and at 733 K with equal weighting after normalizing them to the same maximum intensity.

spectra are shown in Fig. 7. At the lowest temperature a broad structureless line is observed onto which a central feature is superimposed. At room temperature its width is only about half that of the central line of the solid-echo spectrum. The central line here obviously has a different phase than the broad line as evident from the slight undershoots seen near the center. Such apparent phase differences between central and satellite lines were also found in a theoretical analysis when the homonuclear dipolar interactions between the Li spins is taken into account.[24] The Jeener-Broekaert spectra remain virtually unchanged up to 400 K, and then the side maxima of the spectra turn somewhat sharper. Between about 500 and 550 K they become even more pronounced and the central component narrows down significantly. Upon further heating a Pake-like shape emerges onto which a narrow central component is superimposed that contains 1% or less of the total intensity. The residual width of the central line ($\approx$400 Hz) is probably due to the inhomogeneity of our magnet.

The appearance of a Pake-like powder pattern which can be described by a partially averaged *symmetric* ($\eta_Q=0$) quadrupole tensor with a peak to peak separation of 53 kHz ($\delta_Q=2\pi\times 53$ kHz) indicates that more than three inequivalent sites are involved in the ion hopping motion. This is expected on the basis of the disorder in the Si^{4+}/Al^{3+} sublattice. On the other hand, the fast ionic motion which takes place at high temperatures does not average the quadrupolar interaction completely. This indicates that the tensors corresponding to the *finite* number of magnetically inequivalent sites give rise to a preferred orientation within each grain of our polycrystalline specimens.

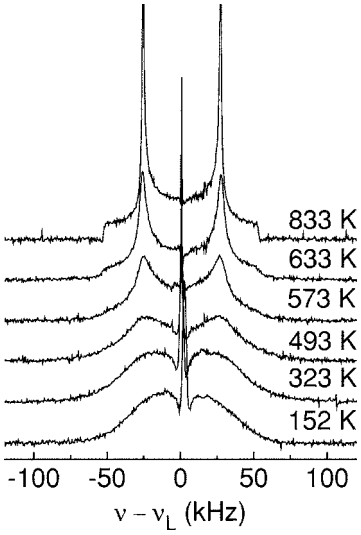

FIG. 7. Temperature dependent spin-alignment spectra of the crystalline phase recorded for $t_p=t_m=10$ μs at 46.1 MHz. All spectra are normalized to exhibit the same maximum intensity.

In Fig. 8 we compare the spin-alignment spectra of the spodumene glass with that of the crystal. Here the trends observed already in the solid-echo spectra (cf. Fig. 5) come out more clearly. The spin-alignment spectra of the glass are significantly broader than those of the crystal. Furthermore, whereas the satellite intensities for the glass tend to vanish at the highest temperatures shown in Fig. 8, those of the crystal exhibit a gradual transition to a Pake powder pattern as discussed above (cf. Fig. 7).

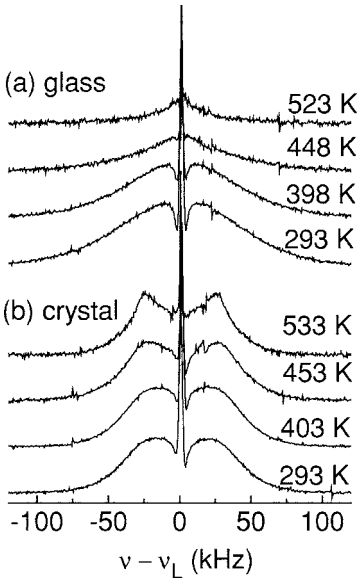

FIG. 8. Comparison of the temperature dependent spin-alignment spectra of (a) glassy and (b) crystalline spodumene for $t_p=t_m=10$ μs at 46.1 MHz.

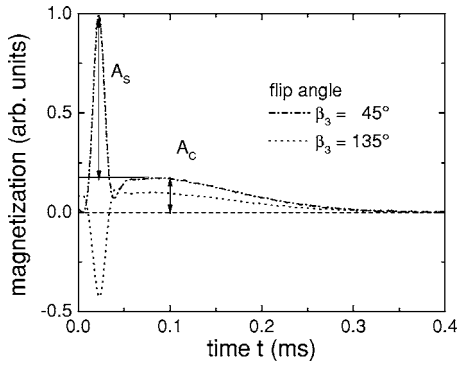

FIG. 9. Time-domain signals generated by a Jeener-Broekaert sequence with the third pulse set to flip angles of $\beta_3=45°$ (dash-dotted line) or 135° (dashed line). The arrows give an impression of how the dipolar (central) and quadrupolar (satellite) contributions to the echo intensity were extracted from the data. The solid line is meant to extrapolate the pedestal to short times. It suggests that the systematic error introduced by reading off A_S at $t=100$ μs and not at the echo center is relatively minor. The data were recorded for crystalline β-spodumene at $T=304$ K with an evolution time $t_p=40$ μs and a mixing time $t_m=0.1$ ms. The Larmor frequency was 117.6 MHz.

In order to study the relative phasing of central and satellite contributions we varied the length of the third pulse. Some results are documented in Fig. 9 where we show the time domain signals recorded for flip angles β_3 of 45° and of 135°. It is seen that the slowly decaying part of the signal, which gives rise to the central part of the spectrum, is very similar for both cases. However, the amplitude of the rapidly decaying quadrupolar part has changed sign upon tripling the pulse length. In order to quantify these effects we recorded the echo heights A_S and A_C, as sketched in Fig. 9, for a wide range of flip angles β_3. In the spectral dimension these amplitudes approximately correspond to the integrated dipolar and quadrupolar intensities. Figure 10 shows that A_S roughly follows a $\sin(2\beta_3)$ dependence as expected on the basis of Eq. (3). The central contribution A_C, on the other hand, exhibits a different behavior which is roughly "mirror symmetric" with respect to flip angles of 90°.

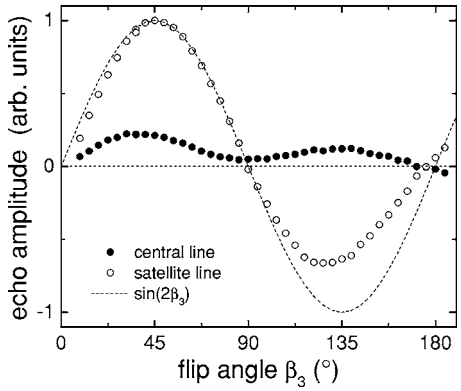

FIG. 10. The amplitudes A_C and A_S, extracted as shown in Fig. 9, are given for a large range of flip angles β_3. For this particular set of data the length of the $\pi/4$ pulse corresponded to 2.0 μs. It is seen that A_S roughly follows a $\sin(2\beta_3)$ dependence, in harmony with what is expected; cf. Eq. (3).

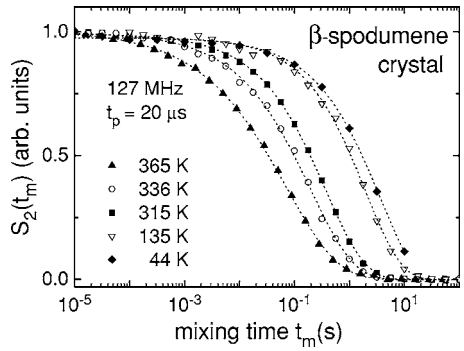

FIG. 11. Decays of the spin-alignment echo amplitudes for crystalline β-spodumene at various temperatures for $t_p=20$ μs and $\omega_L/2\pi=46.1$ MHz. The lines are fits using Eq. (6).

According to the statements summarized in Sec. II, such a behavior could be rationalized if, prior to the third pulse, the relevant product states contained contributions from dipolar coupled ^{7}Li spins that are characterized by odd L. On the basis of the calculation performed in Ref. 24 such terms could arise if coherence transfer pathways are violated, e.g., by relaxation processes. In any case, for large flip angles the systematic evolution during the rf pulses cannot be neglected. The complex effects of soft pulses on nonselectively excited spin-3/2 systems was extensively studied both theoretically and experimentally.[43]

C. Two-time correlation functions

1. Dependence on evolution and mixing times

We measured the stimulated-echo function $S_2(t_p,t_m,t)$ with various of the parameters fixed. Similar to previous studies (cf. Fig. 7 of Ref. 22), we have checked that for $t=t_p$ and for, e.g., $t=t_p+68$ μs the signal contains either dipolar plus quadrupolar contributions or predominantly the dipolar contributions, respectively. Also for spodumene we find a maximum in $S_2(t_p,t_m\to\infty,t_p+68\ \mu\text{s})$ at a time t_D (not shown). From measurements at ten different temperatures it turns out that t_D is related to the FWHM of the dipolar linewidth Δ of the stimulated-echo spectra via $t_D\times\Delta=0.13\pm0.04$. As in our previous investigations, this product is compatible with $(2\pi)^{-1}$ (Ref. 22) and confirms that for sufficiently small t_p the dipolar contributions to the echo need not be taken into account. Thus for $t_p\to0$ one should have a single-particle view on the ion dynamics.

The mixing time dependence of crystalline β-spodumene was measured at 46 MHz for $80\ \text{K}<T<593\ \text{K}$ and at 127 MHz for $35\ \text{K}<T<365\ \text{K}$. In Fig. 11 we present some results recorded at the higher frequency for an evolution time of 20 μs. It is seen that both the time scale and stretching evolve smoothly with temperature. Similar decay curves were obtained at other evolution times. For a description of these data we used a stretched exponential function

$$S_2(t_p,t_m,t_p)=(S_0+S_1\exp\{-[t_m/\tau(t_p)]^{\beta(t_p)}\})\exp(-t_m/T_{1Q}). \tag{6}$$

The offset S_0, the amplitude S_1, the decay constant τ, and the stretching coefficient β in general depend on the evolution

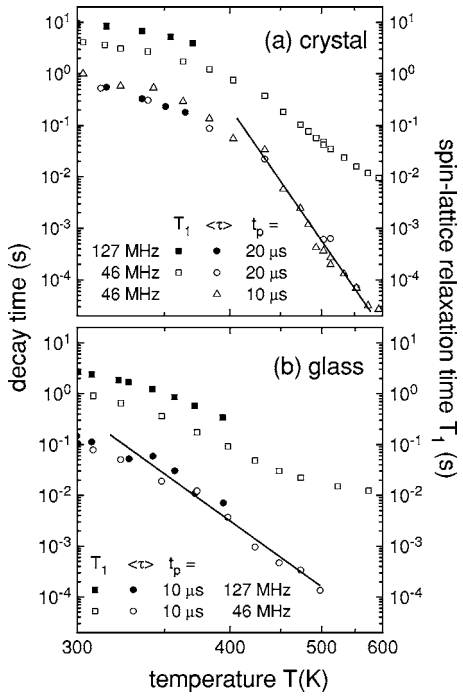

FIG. 12. (a) Mean stimulated-echo decay times $\langle\tau\rangle$ and spin-lattice relaxation times T_1 of crystalline β-spodumene for various evolution times and Larmor frequencies. (b) Analogous plot for glassy spodumene. The representation is chosen such that an Arrhenius law corresponds to a straight line. From the slopes of the lines shown in this figure the energy barriers given in the text were calculated.

time. The second exponential accounts for the decay of the population states (predominantly of the quadrupolar order) during the mixing time. The associated time constant is therefore designated T_{1Q} and should be independent of t_p. For the crystal this was confirmed in a temperature range between 400 and 900 K. Here, at the shortest t_p, a two-step decay was found. The ratio of the spin-lattice relaxation time to the long-time decay was $T_1/T_{1Q} \approx 2.6 \pm 1.0$. At lower temperatures no bimodal decays were detected and therefore T_{1Q} could not be taken into account separately. The time scales and stretching parameters used to describe the data shown in Fig. 11 are discussed below.

2. Time scales and stretching

In order to gain an overview of the spin-alignment measurements, in Figs. 12(a) and 12(b) we collected the fitting parameters as obtained using Eq. (6) for crystalline and glassy spodumene, respectively. Above ambient temperature the time constants exhibit a strong variation as a function of temperature. No Larmor frequency dependence is seen in this range as expected for correlation times characterizing ionic hopping processes.[22,25] In the temperature range covered by Fig. 12, the stretching exponents are constant within experimental error for several Larmor frequencies (not shown). We find $\beta = 0.5 \pm 0.1$ for the crystal and $\beta = 0.3 \pm 0.1$ for the glass. The value even for the crystal is quite small, which may not come unexpected in the light of the observation of two-phase spectra; cf. Fig. 6. The fact that the stretching exponent of the glass is even smaller is consistent with the results for the activation energies E_a obtained from the low-temperature flanks of the spin-lattice relaxation peaks for the glass and the crystal in their high-temperature regimes (see Sec. IV A). Moreover, the strong correlation between β and E_a, pointed out by Ngai and Martin[44] on the basis of ionic conductivity measurements in glasses with various compositions, is fulfilled in the present case of an NMR study in a glass and the corresponding crystalline counterpart.

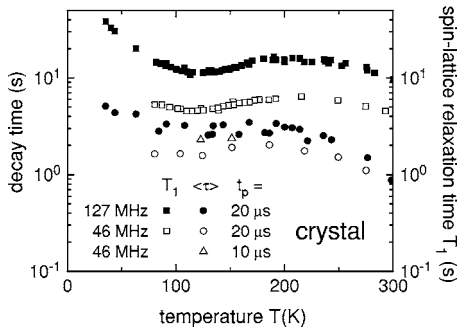

FIG. 13. Stimulated-echo decay times τ and spin-lattice relaxation times T_1 of crystalline β-spodumene for various evolution times and Larmor frequencies. Both quantities τ and T_1 follow the same trend in the temperature range shown here.

As can be recognized from Fig. 13, a frequency dependence emerges for the decay times for temperatures lower than about 300 K. Furthermore, the temperature dependence of the decay times is quite small and resembles that of the spin-lattice relaxation times, which are included in this figure for comparison. In the temperature range below about 50 K the motional correlation times estimated from Fig. 3 should be in the experimental time window (1 ms or slower). Therefore we expected to observe some short-time decay of the two-time correlation function due to the Li^+ hopping within the local double wells. However, no indications for such a decay could be found; cf. Fig. 11 (Ref. 45). We point out that small-amplitude motions in principle are detectable using stimulated-echo spectroscopy.[46] Therefore we speculate that special circumstances in β-spodumene hamper the detection of the two-site jumps. It is known that in β-spodumene the distribution of the local hopping times is very broad, leading to the observation of a nearly constant loss (NCL).[13,14] NCL phenomena were intensively studied for a wide variety of ion conductors in recent years.[47]

For both spodumene modifications the stretching coefficients β show no systematic dependence on frequency and on evolution time (not shown). For $T < 300$ K the exponents signal an apparent narrowing of the stimulated-echo decay (cf. Fig. 11). The temperature dependence of the stretching thus suggests that a mechanism is active which leads to an at least partial averaging of the stimulated-echo decay upon cooling. The situation resembles that of the spin-lattice relaxation in deuteron spin systems, for which spin-diffusion leads to a narrowing of the longitudinal magnetization recovery upon approaching low temperatures;[40] see also the discussion of Fig. 4, above.

We performed stimulated-echo measurements as a function of the evolution time for various temperatures. The

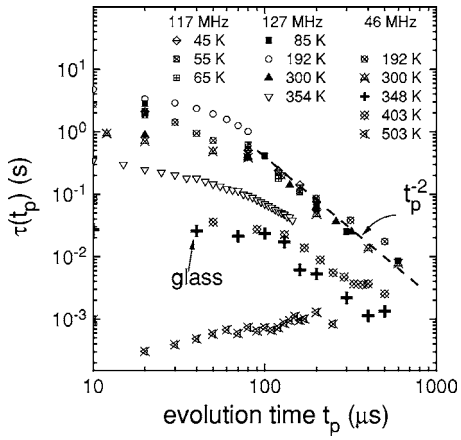

FIG. 14. Mean stimulated-echo decay times $\tau(t_p)$ as a function of the evolution time for various temperatures and Larmor frequencies. At and below room temperature all data in this plot exhibit a quasiuniversal behavior for t_p larger than about 100 μs. This is emphasized by the dashed line. Except for the crosses, all data refer to crystalline β-spodumene.

stretching exponents for crystalline β-spodumene did not show systematic variations with t_p. However, from Fig. 14 it is seen that the decay times typically do exhibit a strong dependence on the evolution time, at low temperatures roughly following a t_p^{-2} behavior. Such a dependence on the evolution time suggests that during the experiment the precession frequencies change in steps that are very small as compared to the linewidth of the rigid lattice spectrum.[42] Two different mechanisms could be responsible for such a spectral diffusion. On the one hand, the charge disorder existing in the glass or, when talking about the crystalline modification, in the Al^{3+}/Si^{4+} sublattice leads to a situation in which the quadrupolar precession frequencies in adjacent Li sites differ only slightly. Then a Li ion performing a long-range hopping process could be characterized by a small-step diffusion process in frequency space. For ions performing two-site jumps no major dependence of the stimulated-echo decay time on the evolution time is expected.[48] At sufficiently low temperatures the hopping correlation times due to long-range ionic transport will turn out to be too long to be seen in the experimental time window of the stimulated-echo experiment and then cannot be held responsible for the t_p^{-2} behavior.

On the other hand, dipolar flip-flop processes among the central transitions which do not require mass transport also lead to small changes of the local precession frequencies. These changes are of the order of the dipolar line width and in a first approximation should be independent of temperature. For first-order quadrupolar perturbations, such that the second-order shifts are much smaller than the dipolar couplings, no dependence on the Larmor frequency should show up. Interestingly in Fig. 14 we observe that the decay times determined for long times indeed exhibit, within experimental error, a universal behavior for $T \leqslant 300$ K (Ref. 49).

For higher temperatures the behavior is different. Although at 354 K the decay times were not measured out to very long evolution times, the data shown in Fig. 14 suggest that the mean decay times are smaller than those corresponding to dipolar flip-flop processes. In this context it should be mentioned that the dipolar coupling as estimated from the width of the central line of the stimulated-echo spectra is practically constant for $T \leqslant 400$ K; see Sec. IV B 2.

At higher temperatures, e.g., $T=503$ K, we find an increase of the decay time with increasing evolution time; cf. Fig. 14. This observation is not completely unexpected since the evolution times are not short as compared to the hopping correlation times, at least for longer t_p. The dynamics taking place during t_p can no longer be neglected under these circumstances. Similar to findings in Ag^+ ion conducting glasses, we interpret this as the signature of a motional phase averaging predominantly affecting the fraction of species moving fast on the scale set by the evolution time.[50] Since in the presence of a distribution of correlation times this fraction obviously increases with increasing t_p, the mean time constant characterizing the slower (than t_p) fraction has to increase.

3. Comparison with measurements of the electrical conductivity

The foregoing discussion allows us to compare the temperature dependent decay times of the glassy with that of the crystalline specimens. In Fig. 12 we present the data in a format which linearizes the Arrhenius law $\tau=\tau_0 \exp(E/k_BT)$, which provides a good description of our data at high temperatures. The solid lines in this figure represent energy barriers of 0.98 ± 0.05 eV for the crystal and 0.58 ± 0.03 eV for the glass. These values can be compared to the ones determined from conductivity measurements which yielded 0.80 eV for the crystal and 0.66 eV for the glass.[4] These numbers essentially agree with the activation energies from the high-temperature sides of the asymmetric peaks in the log T_1^{-1} vs $1/T$ plot (cf. Fig. 1) and confirm that the barriers against long-range hopping transport are lower if the mobile ions move in a *glassy* matrix. Together with the increased stretching of the response in the amorphous phase, this implies that a larger fraction of low-energy barriers is available in the glass.

An estimate of the energy barrier may also be attempted by analyzing the maxima of the spin-lattice relaxation rate T_1^{-1} for several Larmor frequencies. If despite the fact that T_1^{-1} shows non-BPP behavior also for the crystal (cf. Sec. IV A) the BPP condition $\omega_L\tau_C=0.62$ is employed to the crystal T_1^{-1} data of Ref. 3 and of the present work (cf. Fig. 1), we find an energy barrier which is compatible with 1 eV. However, the absolute values of the correlation times estimated using the BPP condition are about a factor of 10 smaller than those extrapolated from the stimulated-echo data. If one assumes a distribution of correlation times, e.g., of the Cole-Davidson type, for which the spectral density $J_{CD}(\omega)=\omega^{-1}(1+\omega^2\tau^2)^{-\beta_{CD}/2}\sin[\beta_{CD}\arctan(\omega\tau)]$ is characterized by the width exponent β_{CD}, then $\omega_L\tau_C$ at the T_1^{-1} maximum in general deviates from 0.62. For $\beta_{CD}=0.3$, say, at the T_1^{-1} maximum $\omega_L\tau_C$ is 2 times larger, thus somewhat mitigating, but not fully resolving the seeming discrepancy.

V. SUMMARY

In the present article we employed various NMR methods to study the dynamics of the Li^+ ions in a crystalline and in

the glassy form of spodumene. Previous measurements of the spin-lattice relaxation rates of these aluminosilicates have been extended the experiments to higher Larmor frequencies as well as to lower temperatures. The latter was important because direct evidence for local spin-lattice relaxation rate maxima was obtained. The behavior of these peaks in the relaxation rate was compared with the evolution of dielectric loss peaks and reasonable agreement was found. This confirms the previous assignment that the dielectric relaxation process is due to a local Li^+ hopping in double-well potentials. For the glassy material indications for such a feature did not show up in the present data.

In order to obtain solid-echo spectra with reduced distortions and also with the proper amplitude ratio of central and to satellite transitions, we used a 90°-64° sequence in the experimental part of this work. Justification for this choice was given on the basis of a simple density matrix calculation. By comparing the experimental solid-echo spectra with the stimulated-echo spectra for a large temperature range, we found that the central transition of the latter is substantially smaller. The larger variability of the local ion environment of the Li species in the glass as compared to that in the crystal is directly reflected in the shape of the spectra.

Then the impact of the nuclear dipole-dipole interactions on the stimulated-echo spectra and on the corresponding time-domain experiments was investigated. To this end we analyzed a large number of experiments for which the evolution and the mixing times were varied. On the basis of measurements carried out in a wide temperature range and for several Larmor frequencies, we discussed the conditions under which ion hopping correlation functions can be extracted from our data. The hopping correlation function thus obtained may be viewed as the long-time analog of the intermediate incoherent scattering function which probes the dynamics on the length scale of the typical Li-Li distance.

Our stimulated-echo experiments enabled us to determine correlation times for the hopping motion in a large temperature range. Near and above room temperature we found thermally activated behaviors and for each modification—glassy and crystalline—the energy barriers against long-range ionic transport could be identified. The energy barriers exhibit a considerable distribution as can be inferred from the significant stretching of the hopping correlation functions. Our experiments show that the latter is more pronounced in the glass as compared to the crystal and correlated with the corresponding activation energies obtained from the spin-lattice relaxation experiments.

Using the stimulated-echo method, so far it has not been possible to detect any indications of the local Li ion hopping in the ultraslow regime. On the other hand, the modulation of the electrical field gradient at the Li site, which is associated with this two-site jump, is sufficient to lead to a signature in the spin-lattice relaxation rate near 120 K. From dielectric spectroscopy it is known that this process, which at 40 to 50 K is in the milliseconds to seconds regime, is governed by a broad distribution of energy barriers. Since the width of the associated distribution of correlation times is inversely proportional to temperature, this may rationalize the failure to observe this two-site jump using the stimulated-echo method at relatively low temperatures.

ACKNOWLEDGMENTS

We are indebted to Professor Dr. Otmar Kanert for stimulating discussions over the years. Most of the experimental work reported in this article was carried out at the Institut für Physikalische Chemie, Universität Mainz. We thank H. W. Spiess for sharing a high-temperature probe head, and K. R. Jeffrey as well as B. Geil for valuable suggestions concerning the manuscript. The financial support for this project provided by the Deutsche Forschungsgemeinschaft (Grant No. Bo1301/5) and by the Graduiertenkolleg 298 (Dortmund) is highly appreciated. Part of the work done at the Institut für Physikalische Chemie und Elektrochemie, Universität Hannover, was financed by the Sonderforschungsbereich 173 of the Deutsche Forschungsgemeinschaft.

*FAX: +49-231-755-3516. Electronic address: Roland.Bohmer@Uni-Dortmund.de

†Electronic address: heitjans@pci.uni-hannover.de

[1] R. Roy, D. M. Roy, and E. F. Osborn, J. Am. Ceram. Soc. **33**, 152 (1950).

[2] W. Pannhorst, R. Haug, E. Rodek, and K. Stetter, J. Non-Cryst. Solids **131–133**, 488 (1991).

[3] W. Franke and P. Heitjans, Ber. Bunsenges. Phys. Chem. **96**, 1674 (1992).

[4] B. Munro, M. Schrader, and P. Heitjans, Ber. Bunsenges. Phys. Chem. **96**, 1718 (1992).

[5] D. Brinkmann, Prog. Nucl. Magn. Reson. Spectrosc. **24**, 527 (1992).

[6] P. Heitjans and S. Indris, J. Phys.: Condens. Matter **15**, R1257 (2003).

[7] C.-T. Li and D. R. Peacor, Z. Kristallogr. **126**, 46 (1968).

[8] G. Roth and H. Böhm, Solid State Ionics **22**, 253 (1987).

[9] P. Heitjans, A. Schirmer, and S. Indris, in *Diffusion in Condensed Matter—Methods, Materials, Models*, edited by P. Heitjans and J. Kärger (Springer, Berlin, in press).

[10] P. Heitjans, W. Faber, and A. Schirmer, J. Non-Cryst. Solids **131–133**, 1053 (1991).

[11] A. Nordmann, Y. Cheng, T. J. Bastow, and A. J. Hill, J. Phys.: Condens. Matter **7**, 3115 (1995).

[12] M. C. Jermy, G. N. Greaves, M. E. Smith, G. BushnellWye, A. C. Hannon, R. L. McGreevy, G. Derst, and B. Tilley, Mater. Sci. Forum **228**, 537 (1996).

[13] A. K. Rizos, J. Alifragis, K. L. Ngai, and P. Heitjans, J. Chem. Phys. **114**, 931 (2001).

[14] R. Böhmer, M. Lotze, P. Lunkenheimer, F. Drexler, G. Gerhard, and A. Loidl, J. Non-Cryst. Solids **172–174**, 1270 (1994).

[15] R. Böhmer, P. Lunkenheimer, M. Lotze, and A. Loidl, Z. Phys. B: Condens. Matter **100**, 583 (1996).

[16] W. Franke, P. Heitjans, B. Munro, and M. Schrader, in *Defects in Insulating Materials*, edited by O. Kanert and J.-M. Spaeth (World Scientific, Singapore, 1993), p. 1009.

[17] K. L. Ngai, J. Chem. Phys. **98**, 6424 (1993). For a discussion of other glasses, see also M. Tatsumisago, C. A. Angell, and S. W. Martin, J. Chem. Phys. **97**, 6968 (1992).
[18] R. Winter, K. Siegmund, and P. Heitjans, J. Non-Cryst. Solids **212**, 215 (1997).
[19] G. Morrison, C. M. Barker, K. M. Kennedy, and A. V. Chadwick, Mater. Sci. Forum **239**, 417 (1997).
[20] J. Jeener and P. Broekaert, Phys. Rev. **157**, 232 (1967).
[21] E. Göbel, W. Müller-Warmuth, H. Olyschläger, and H. Dutz, J. Magn. Reson. (1969-1992) **36**, 371 (1979).
[22] F. Qi, T. Jörg, and R. Böhmer, Solid State Nucl. Magn. Reson. **22**, 484 (2002).
[23] R. Böhmer, T. Jörg, F. Qi, and A. Titze, Chem. Phys. Lett. **316**, 417 (2000).
[24] F. Qi, G. Diezemann, J. Lambert, H. Böhm, and R. Böhmer, J. Magn. Reson. **169**, 225 (2004).
[25] M. Wilkening and P. Heitjans, Defect Diffus. Forum **237–240**, 1182 (2005).
[26] M. Eden and L. Frydman, J. Chem. Phys. **114**, 4116 (2001).
[27] G. D. Bowden, W. D. Hutchison, and J. Khachan, J. Magn. Reson. (1969-1992) **67**, 415 (1986).
[28] H. Abe, H. Yasuoka, and A. Hirai, J. Phys. Soc. Jpn. **21**, 77 (1966).
[29] X.-P. Tang, R. Busch, W. L. Johnson, and Y. Wu, Phys. Rev. Lett. **81**, 5358 (1998).
[30] R. Böhmer, J. Magn. Reson. **147**, 78 (2000).
[31] M. Vogel, Phys. Rev. B **68**, 184301 (2003).
[32] C. Jäger and G. Scheler, Exp. Tech. Phys. (Berlin) **32**, 315 (1984).
[33] N. Bloembergen, E. M. Purcell, and R. V. Pound, Phys. Rev. **73**, 679 (1948).
[34] T. Blochowicz, A. Kudlik, S. Benkhof, J. Senker, E. Rössler, and G. Hinze, J. Chem. Phys. **110**, 12011 (1999).
[35] R. Böhmer and F. Kremer, in *Broadband Dielectric Spectroscopy*, edited by F. Kremer and A. Schönhals (Springer, Berlin, 2002), pp. 625–684.
[36] O. Kanert, R. Küchler, K. L. Ngai, and H. Jain, Phys. Rev. B **49**, 76 (1994).
[37] M. Meyer, P. Maass, and A. Bunde, J. Non-Cryst. Solids **172–174**, 1292 (1994).
[38] A. Bunde, W. Dieterich, P. Maass, and M. Meyer, in *Diffusion in Condensed Matter—Methods, Materials, Models*, edited by P. Heitjans and J. Kärger (Springer, Berlin, in press).
[39] E. R. Andrew and D. P. Tunstall, Proc. Phys. Soc. London **78**, 1 (1961).
[40] W. Schnauss, F. Fujara, and H. Sillescu, J. Chem. Phys. **97**, 1378 (1992).
[41] The spectrum of a sample with a ^{7}Li:^{6}Li ratio of 1:3 was very similar.
[42] R. Böhmer, G. Diezemann, G. Hinze, and E. Rössler, Prog. Nucl. Magn. Reson. Spectrosc. **39**, 191 (2001).
[43] P. P. Man, Mol. Phys. **72**, 321 (1991); J. Magn. Reson. (1969-1992) **100**, 157 (1992); L. Pandey, M. Kotecha, and D. G. Hughes, Solid State Nucl. Magn. Reson. **16**, 261 (2000).
[44] K. L. Ngai and S. W. Martin, Phys. Rev. B **40**, 10550 (1989).
[45] It cannot be ruled out that the typical difference of the NMR frequencies associated with the two sites is too small to be resolved with the short evolution times used in Fig. 11. In order to increase the sensitivity of the stimulated-echo experiment we carried out low-temperature measurements ($30\ \mathrm{K} < T < 50\ \mathrm{K}$) for a range of evolution times extending up to $t_p = 160\ \mu$s. However, no indications for the sought two-sites jump could be detected.
[46] M. Vogel and E. Rössler, J. Chem. Phys. **114**, 5802 (2001).
[47] See, e.g., O. Kanert, R. Küchler, P. C. Soares, and H. Jain, J. Non-Cryst. Solids **307–310**, 1031 (2002) and references cited therein.
[48] F. Qi, M. Winterlich, A. Titze, and R. Böhmer, J. Chem. Phys. **117**, 10233 (2002).
[49] Almost temperature (but not evolution time) independent correlation times were also reported from deuteron NMR in the β-relaxation regime of glassy systems; cf. Fig. 9 of Ref. 46.
[50] S. Berndt, K. R. Jeffrey, R. Küchler, and R. Böhmer, Solid State Nucl. Magn. Reson. **27**, 122 (2005).